Proposal for a new research grant:

Dynamic Electrowetting at Nanoporous Surfaces: Switchable Spreading, Imbibition, and Elastocapillarity

Applicant

Prof. Dr. rer. nat. Patrick Huber
Institut für Materialphysik
Technische Universität Hamburg (TUHH)

1 State of the art and preliminary work

1.1 State of the art

Electrowetting allows a reversible control of the wetting behaviour and the spreading dynamics of liquid electrolytes at surfaces[1–4] and interfaces.[5] For ideal, planar electrically-conductive surfaces of metals and semi-conductors, e.g. gold and highly-doped silicon surfaces, an extensive fundamental understanding of the static and dynamic electrowetting behaviour has been attained over the last 50 years.[2,4] The electrostatic forces induce contact angle changes and thus can result via changes in the Laplace pressure in the liquids to motion of entire droplets.[6] However, it turned out as well that theories had to be extended to account for distortions of the liquid surface due to local electric fields, for the finite penetration depth of electric fields into the liquid, as well as for finite conductivity effects in alternating-current (AC) experiments.[2,4] Microstructured surfaces can result both in continuous transitions between different droplet shapes, but also to discontinuous morphological transitions between distinct liquid morphologies.[2]

The governing phenomenological description at planar surfaces refers to the Lippmann equation,[7] i.e. the solid-electrolyte interfacial tension, σ_{SL}, obeys $d\sigma_{SL} = -q\ dE$ with q the charge density (charge per unit area). As the capacitance is always positive, the surface tension is at maximum at the potential of zero charge (PZC), where $q = 0$. The decrease in σ_{SL} upon charging will enhance the wetting. This is a well-known consequence of the Young equation, $\cos\Theta = \sigma_{SV} - \sigma_{SL}/\sigma_{LV}$, where σ_{SV} is the solid-vapour interface energy. Thus, a maximum in Θ is expected at the PZC.

Electro-chemical reactions at planar electrolyte-solid interface, most prominently oxidation and reduction of the surface, can also result in changes in the fluid-wall interaction and thus in changes in the wetting conditions. This can be circumvented by the introduction of dielectric layers between electrolyte and electrically conductive substrate, i.e. a electrowetting-on-dielectric (EWOD) geometry.[2] The EWOD is nowadays often used, since it allows for much larger potential windows, i.e. the smallest and largest applicable electrical voltage without chemical reactions and the resulting Faradaic currents. Thus, the wetting energy changes are much larger.[2,4]

Much less, however, is known about the validity of fundamental electrowetting concepts in the case of nanoporous surfaces, as they are e.g. nowadays readily available in the form of nanoporous silicon,[11] gold[12] or carbon[13] materials. Here a simultaneous spreading of the macroscopic triple-line at the outer circumference[3] with the formation and movement of nanoscale menisci and precursor films ahead of the menisci[14,15] in the substrate pores arises, see illustration and detailed illustration of an electrowetting experiment at a model nanoporous surfaces, i.e. a planar silicon substrate traversed by parallel tubular nanopores along the substrate normal in Fig. 1. Here, the liquid imbibition into the nanofluidic geometry and the droplet spreading at the substrate surface compete. This gives rise to a potentially complex droplet spreading, electrokinetic- and imbibition kinetics.[16–19]

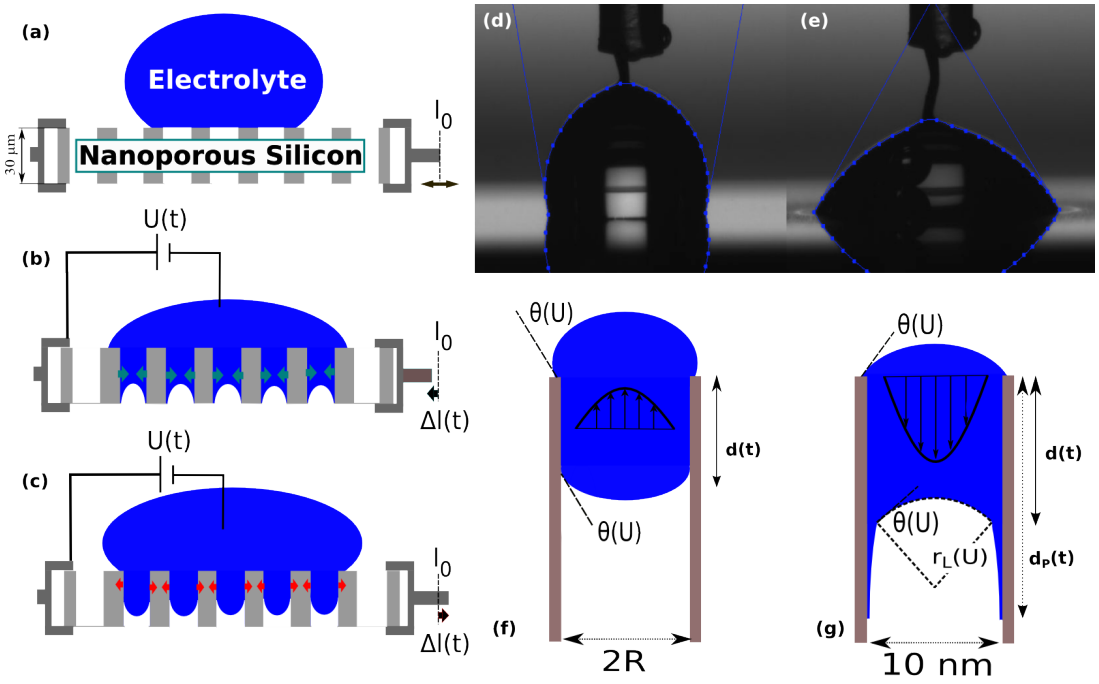

Figure 1: Schematic sideview on a dynamic electrowetting and elastocapillarity experiment at a model nanoporous solid membrane: (a) Initial Cassie-Baxter state where a droplet is sitting on a silicon substrate traversed by a parallel array of cylindrical nanopores (contact angle of the liquid with regard to the substrate surface in the absence of an external electrical potential $\theta(U = 0\ V) > 90°$). (b) Wenzel state with $\Theta(U) < 90°$ both at the macroscopic substrate surface and in the nanopores. This results in droplet spreading at the substrate surface and electrolyte imbibition into the nanopores: Highly curved concave menisci have advanced to a depth $d(t)$ after a step-wise application of an electrical potential U, see also panel (g) for an illustration of the dynamic wetting situation in a single nanochannel. There also a pre-cursor film is indicated. c) The nanopore menisci are receding after the electrowetting conditions have been switched to $\Theta(U) < 90°$ after an initial pore filling process, see also pane (f) for an illustration of the dynamic dewetting situation in a single nanochannel. Both in (b) and (d) the Laplace pressure in the liquid result in a dynamic manner to traction forces at the pore walls (indicated by green and red arrows) and thus to a filling-dynamics dependent macroscopic deformation[8,9] of the silicon membrane $\Delta l(t)$: Upon pore filling the concave advancing menisci result in negative, tensile pressures in the liquid and thus in a contraction of the membrane. Upon pore emptying the convex, receding menisci result in positive hydrostatic pressures in the electrolyte and thus in an expansion of the membrane. Static electrowetting experiment with an aqueous electrolyte (2 M KCl solution) on nanoporous silicon: (d) No electrical potential, contact angle $\Theta = 101.3°$. (e) under negative electrical potential $\Theta = 54.3°$. The droplet shape analysis, in particular the determination of the contact angle, see blue lines, is performed by the DropAnalysis plugin of ImageJ.[10] Note that different length scales were chosen for the illustration of the macroscopic droplet as well as the membrane in comparison to the nanoscale pores and the confined liquid.

The spreading kinetics of partially wetting droplets of simple liquids (without electrical stimulus) on top of porous media have been explored by analytical models, Molecular Dynamics and Lattice Boltzmann simulations.[20–22] In particular Seveno *et al.*[20] provide detailed dynamical scaling laws for the contact angle dynamics $\Theta(t)$, the sessile drop radius and the droplet volume upon spreading and simultaneous liquid imbibition at a surface permeated by arrays of parallel tubular non-interconnected channels, as suggested as experimental model system in this proposal. The authors validate their analytical hydrodynamical considerations by Molecular Dynamics simulations for a Lennard-Jones fluid and arrays of nanochannels 7.5 nm across. The results show a power-law evolution of the wetted zone radius with time, both exponent and prefactor decreasing with increasing porosity of the surface. The evolution of the droplet radius in time emerges from a competition between pure droplet spreading and capillary imbibition in the porous medium resulting in a non-monotonous evolution of the droplet radius, see Fig. 2. One goal of the experiments proposed below is a validation of these theoretical considerations.

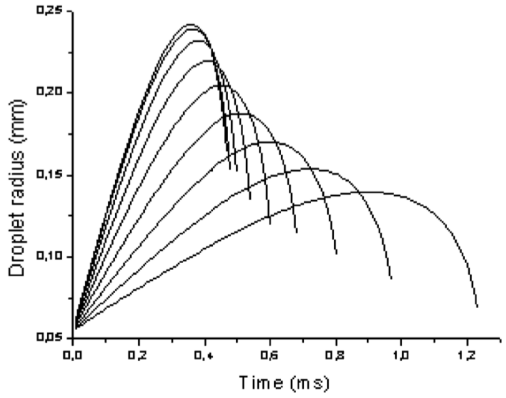

Figure 2: Time-evolution of the base radius of a droplet sitting on a planar surface traversed by an array of parallel non-interconnected channels as predicted within an analytical hydrodynamic model by Seveno *et al.*.[20] The initial, non-equilibrium contact angle is 180°. From top to bottom the solid equilibrium angle is 0, 10, 20, ..., 80 °.

Seveno *et al.* assume that the imbibition kinetics can be described by lamellar liquid flow into a cylindrical capillary at low Reynolds numbers.[23,24] According to this classical scenario, the molecular layer of the flowing liquid in direct vicinity of the capillary wall is immobilized ("no-slip velocity boundary condition"). The imbibition kinetics can then be described by the classic Lucas-Washburn (LW)–equation $d^2(t) = v_i \cdot t$, where $d(t)$ is the meniscus position and t the elapsed duration of capillary filling,[25,26] see Fig. 1. The imbibition speed v_i results from a balance of capillary forces and the viscous drag in the liquid column behind the meniscus. While the dependence of $d(t)$ on $\sqrt{t}$ appears to be universal and has also been found for pores a few nanometer across,[27] the prefactor v_i has remained a matter of debate.[15] Experimental[24,27–30] and theoretical studies[4,31,31–35] of Hagen-Poiseuille capillary flow indicate continuum-like fluid behaviour down to very small length scales for simple liquids. However, if the capillary diameters are reduced to values between a few nm, long-range molecular interactions such as van der Waals forces, thermal fluctuations, and hydrodynamic slippage, which are irrelevant at the micrometer scale and above, may prevail over macroscopic hydrodynamic effects[36,37] and thus result in changed imbibition speeds as compared to the prediction based on macroscopic hydrodynamics. For example, simulation[38] and experimental studies,[27,29] have demonstrated that for simple wetting liquids sticky boundary layers occur due to strongly adsorbed monolayers. They effectively reduce the "hydraulic" pore diameter compared to the "nominal" one, as determined for example by volumetric sorption isotherm measurements. Moreover, hints of thin precursor films in the nanopores, ahead of the advancing menisci, similarly as known from droplet wetting at planar surfaces[39,40] have been inferred from Molecular Dynamics simulations[14] and found in experiments on polymer imbibition in nanochannels,[15] see an illustration of a spreading precursor film at the pore wall, ahead of the nanoscale meniscus Fig. 1(g). Interestingly, also the spreading kinetics of the precursor film in the nanopores is predicted to follow a $\sqrt{t}$-kinetics,[14] which has not been confirmed experimentally up until now.

Note that during the initial stage of imbibition, the liquid molecules are accelerated from the quiescent state to classical Lucas-Washburn dynamics, and the menisci characteristic of the imbibition front form. For pre–LW imbibition stages, the imbibition front propagation scales with t (cf. Table 1

in Ref. 41). According to classical hydrodynamics, the duration of this initial imbibition regime, characterised by the competition of the guest's inertia and interfacial interactions, is described by a characteristic time $\tau^* \sim \rho r^2/(4\eta)$ (ρ, density of liquid; r, pore radius; η, viscosity of liquid).[42] For nanopores this inertia-determined time scale is on the ns time scale, well below the time scales accessible in the experiments envisioned here.[27]

There are a few experimental studies on wetting and/or spontaneous imbibition of electrically-switchable nanoporous substrates, most prominently carbon nanotube membranes[13] and aligned carbon nanotube films.[43,44] These studies remained rather on a phenomenological level and were aimed at a principal demonstration of switchable electrowetting, e.g. of the transition between a non-wetting, Cassie-Baxter state and a partially wetting Wenzel state on these textured substrates. No details on the liquid invasion kinetics are resolved in these experiments. Thus, to the best of our knowledge, no rigorous experiments aimed at a detailed study of the fluid dynamics at nanoporous surfaces under electrical potential control have been reported so far.

In liquid-filled nanoporous media huge negative or positive Laplace pressures $p_L = 2\sigma_v l/r$ on the order of several 10 MPa can occur because of highly curved liquid-vapour menisci with nanoscale curvature radii r. This results in traction forces on the pore walls and subsequent in macrosopic strains in the nanoporous medium.[8,45] Such elastocapillarity effects have been successfully explored theoretically and experimentally at planar soft surfaces and in more complex solid-fluid geometries,[46–49] e.g. fibre wetting geometries. Similarly, a substantial predictive understanding of this phenomenon for liquids confined in nanoporous media has been achieved over the last ten years,[45,50] in particular also for liquids condensed in nanoporous silicon, see Ref.[8,51] and the description of our preliminary work on elastocapillarity in the section on our preliminary work below. In the experiments suggested here these traction forces build up and vanish dynamically as a function of liquid (de)wetting and the corresponding Laplace pressures, i.e. the menisci radii are under external potential control $r = r(U)$ via the electrically adaptable wetting energies, see Fig. 1 for an illustration of this effect. Thus electrically-switchable, dynamic elastocapillarity is expected to occur in our experimental system. Note however, that the expected strains ϵ and thus silicon pore diameter changes are on the order of 10^{-4}.[8] Thus, they are purely elastic and a complex coupling of the elastocapillarity dynamics to the imbibition hydrodynamics,[52] in the sense of changing hydraulic flow radii upon fluid invasion, is negligible. This significantly reduces the complexity of the study of elastocapillarity and makes stiff silicon membranes particularly suitable for a fundamental study of switchable elastocapillarity at the nanoscale.

1.2 Preliminary work

The main focus of the Huber research group is the physical behaviour of molecular liquids confined in nanoporous media. Thermodynamic equilibrium phenomena, such as capillary condensation, crystallisation, phase transition and self-assembly behaviour have been studied in the past.[56,57] For a number of years also non-equilibrium phenomena, such as gas flow, imbibition and imbibition front broadening have been explored as a function of the complexity of the building blocks of the condensates, ranging from simple rare gas fluids via n-alkanes and water to polymers. These experimental studies profited from an extensive expertise in the preparation and tailoring of nanoporous media, most prominently nanoporous silicon with self-organised, aligned tubular channels[54,57,58] arranged in a short-range hexagonal manner and tunable in terms of their fluid-pore interactions by surface grafting methods, such as oxidation of the pore walls and silanization.[58,59] Recent achievements were the demonstration of the validity of the Lucas-Washburn imbibition dynamics for a variety of liquids (water and a selected set of linear hydrocarbons ranging from C_8H_{18} up to $C_{32}H_{66}$) in pores of $\sim$10 nm diameter by gravimetric and neutron imaging experiments on monolithic mesoporous materials (silica, silicon and nanoporous gold).[12,27,59–63]

Moreover, complementary quasi-elastic neutron scattering measurements were performed. These

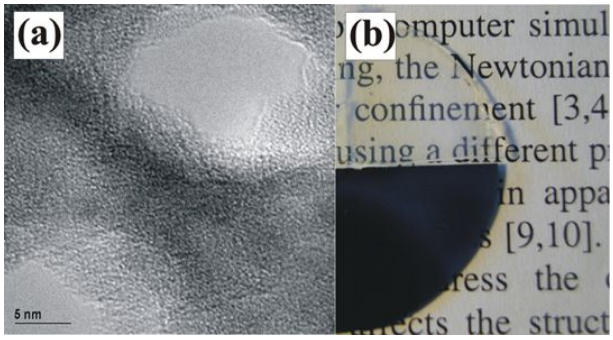

Figure 3: (a) Transmission electron micrographs of pore entrances in nanoporous silicon, electron beam parallel to <100> crystallographic direction of silicon.[53,54] (b) Pictures of free standing membranes of silicon (bottom) and silica (top), which are permeated by an array of linear pores of $\approx$ 10 nm pore diameter and 200 μm length. The monolithic silica membrane can be prepared by thermal oxidation of the electrochemically prepared mesoporous silicon membrane.[55]

measurements are sensitive to the molecular self-diffusion in the pores (characteristic of thermal equilibrium) and thus via the Stokes-Einstein relation also to the viscosity (characteristic of non-equilibrium). In agreement with conclusions from the capillary rise experiments a partitioning of the mobility of the molecules in the pores was found: One component with a bulk-like self-diffusion dynamics in the center of the pores and a second one which is immobile on the time scale probed in the neutron scattering experiment.[64,65] It is understood that for channels a few nanometers across such sticky, adsorbed molecular layers significantly decrease the overall hydraulic permeability of a nanoporous membrane. Therefore, the knowledge of their existence and how to systematically manipulate their characteristics is of utmost importance and could be also of relevance for the project proposed here.

Within a Diploma thesis and several Master thesis also the wetting dynamics of water and simple liquids, such a liquid n-alkanes and alcohols have been explored in thin films of nanoporous silicon. To track the invasion front an optical interferometric method was employed, see Fig.4.[66,67] Due to the invasion of the liquid into the nanoporous silicon, constructive and destructive interference of reflected laser light occurs which can directly be translated to the capillarity-driven liquid advancement in the nanoporous medium with a high spatial (sub-μm) and high temporal resolution (μs).

Of peculiar relevance for the present project are also experiments on switchable, direct electrowetting of nanoporous gold samples. It could be demonstrated that in nanoporous gold an active control of the spontaneous imbibition process (acceleration and arrests of the imbibition front) can be reversibly achieved by externally applied electrical fields and thus by changes of the electrolyte-host interactions.[12] Huge hysteresis in the imbibition dynamics were traced to network effects in the complex sponge-like pore space of nanoporous gold. See Fig. 5 for electrical-potential dependent imbibition dynamics experiments.[12] Moreover, potential-step coulometry experiments allowed to study the charge kinetics in the metallic nanopores and the determination of the electrical capacity of the nanoporous metallic sponges.

Promising, preliminary experiments with regard to the project proposed here were performed within an ongoing Bachelor thesis on electro-wetting of aqueous electrolyte solutions (2 M KCl) on p-doped nanoporous silicon membranes. See Fig. 1 for side-view pictures recorded of a droplet under electrical potential control and controlled atmosphere. In a direct electrowetting experiment the contact angle could be changed from the Cassie-Baxter state ($\Theta = 101.3°$) to the Wenzel state ($\Theta = 54.3°$). Cyclic voltammetry on bulk silicon indicated no irreversible surface modification in the applied potential window. In previous studies, presented in WP 1.2 also the imbibition dynamics into the nanoporous silicon was successfully recorded in this geometry.[66]

Elastocapillarity experiments on nanoporous silicon were performed during in-situ monitoring of the

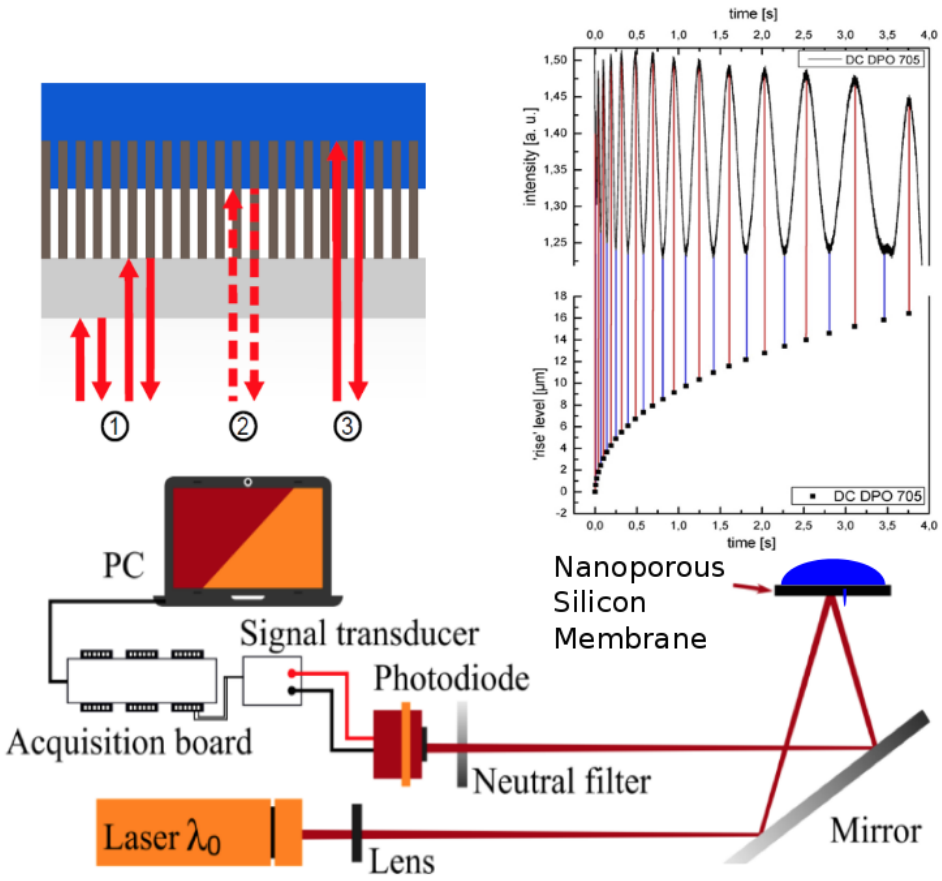

Figure 4: Opto-interferometrical monitoring of the filling of a nanoporous silicon membrane. Left panel: Schematic sketch of the experimental setup along with an illustration of the occurrence of Laser light interferences by the back reflection at different interfaces during movement of a liquid front in a thin porous plate permeated by a parallel array of tubular channels (nanoporous silicon). Right panel: Intensity of reflected Laser light as a function of time during capillarity-driven water flow in nanoporous silicon (10 nm pore diameter) and the corresponding, calculated position of the liquid front in pore space. The infiltration kinetics follows the classic Lucas-Washburn $\sqrt{t}$-law. Diploma Thesis of Mark Busch[66] and PhD thesis of L. Cencha (in preparation).

macroscopic membrane deformation upon water condensation, in particular water film formation at the pore walls and subsequent capillary condensation.[8] The tensile Laplace pressure in the nanopores was externally controlled via the water vapour pressure, see Fig. 6. This experiments were analysed with phenomenological thermodynamical and continuum-mechanics models for sorption strains in nanopores (Kelvin-Laplace equation and poroelastic models) and allowed for detailed insights in the elastocapillarity of nanoporous silicon.[8,9] Thus, these experiments build a sound base for the dynamic elastocapillarity experiments under electrowetting conditions suggested here.

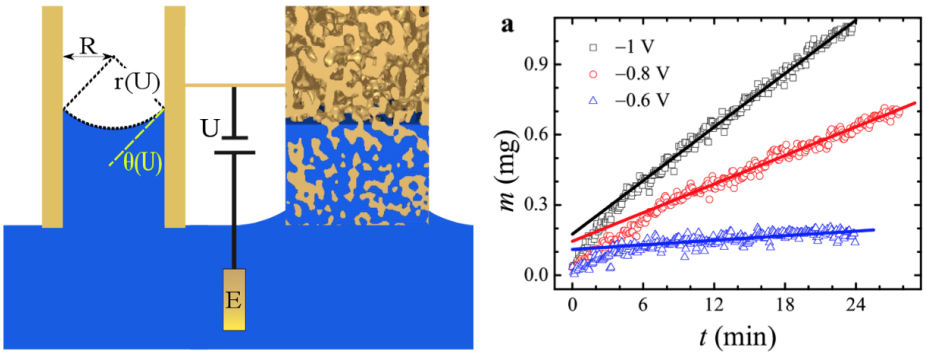

Figure 5: Imbibition of aqueous solution in nanoporous gold under electrical potential control of the liquid-solid interfacial tension: (left) Comparison of the electro-imbibition geometry in a single cylindrical gold capillary, where the liquid forms a concave meniscus with curvature radius $r(U)$, resulting from a potential U-dependent contact angle $\Theta(U)$ in comparison with the capillary rise phenomenology in 3D bicontinuous nanoporous gold under direct electrowetting conditions. (right) Experimental demonstration of switchable electro-capillary rise in nanoporous gold - Mass uptake of the porous host, m, versus time, t, for experiments at various constant values of the electrode potential, as indicated by labels.[12]

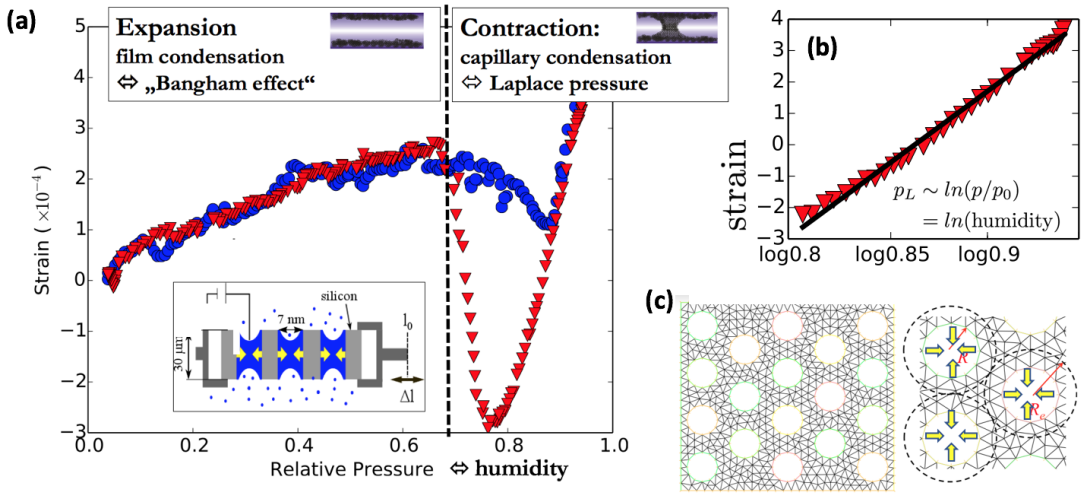

Figure 6: Elastocapillarity upon water adsorption and capillary condensation in a nanoporous silicon membrane: (a) Macroscopic in-plane strain $\epsilon_{||}$ as a function of increasing (blue symbols) and decreasing (red symbols) water vapour pressure (humidity). For small water vapour pressures (below 70% humidity) the membranes expands because of the formation of adsorbed water monolayers at the nanopore walls. The water adsorption reduces the solid-vapour interfacial tension. Each pore expands and thus the entire membrane expands (Bangham regime,[45,68]). At around 70% humidity capillary condensation and thus the formation of highly curved concave menisci occurs in pore space. The resulting Laplace tensile pressures result in tensile traction forces on the solid pore walls, see inset in panel (a) and thus to an in-plane contraction of the entire membrane.[8] (b) In the capillary-condensed regime the liquid menisci curvatures and thus the Laplace tensile pressure in the nanopores depend according to the Laplace-Kelvin equation logarithmically on the vapour pressure resulting in a strain which is a linear function of the logarithm of the vapour pressure. (c) The simple hexagonal arrangement of the pores in nanoporous silicon allow one to achieve a full quantitative understanding of the deformation of the matrix both in finite-element simulations and continuum-models for elastocapillarity.[8,9]

.

1.3 Project-related publications

1) S. Gruener and **P. Huber**: *Capillarity-driven oil flow in nanopores: Darcy scale analysis of Lucas-Washburn imbibition dynamics*, Transport in Porous Media (in press, 2018).

2) G.Y. Gor, **P. Huber**, and J. Weissmueller: *Elastocapillarity in nanopores: Sorption strain from the actions of surface tension and surface stress*, Phys. Rev. Mat. 2 (2018) 086002.
3) S. Gruener, D. Wallacher, S. Greulich, M. Busch, and **P. Huber**: *Hydraulic transport across hydrophilic and hydrophobic nanopores: Experiments with water and n-hexane*, Phy. Rev. E 93 (2016) 013102.
4) **P. Huber**: *Soft matter in hard confinement: phase transition thermodynamics, structure, texture, diffusion and flow in nanoporous media*, J. Phys.: Cond. Matt. 27 (2015) 103102.
5) G. Gor, L. Bertinetti, N. Bernstein, P. Fratzl, and **P. Huber**: *Elastic response of mesoporous silicon to capillary pressures in the pores*, Appl. Phys. Lett. 106 (2015) 261901.
6) Y. Xue, J. Markmann, H. Duan, J. Weißmüller, **P. Huber**: *Switchable imbibition in nanoporous gold*, Nat. Commun. 5 (2014) 4237
7) S. Gruener, Z. Sadjadi, H.E. Hermes, A.V. Kityk, K. Knorr, S.U. Egelhaaf, H. Rieger, **P. Huber**: *Anomalous front broadening during spontaneous imbibition in a matrix with elongated pores*, Proc. Nat. Acad. Sci. (PNAS) USA 26 (2012) 10245.
8) S. Gruener and **P. Huber**: *Spontaneous imbibition dynamics of an n-alkane in nanopores: Evidence of meniscus freezing and monolayer sticking*, Phys. Rev. Lett. 103, 174501 (2009).
9) S. Gruener, T. Hofmann, D. Wallacher, A. Kityk and **P. Huber**: *Capillary rise of water in hydrophilic nanopores*, Phys. Rev. E 79, 067301 (2009).
10) S. Gruener and **P. Huber**: *Knudsen diffusion in silicon nanochannels*, Phys. Rev. Lett. 100, 064502 (2008).

2 Objectives and work programme

2.1 Anticipated total duration of the project

3 years

2.2 Objectives

Electrically conductive substrates, such as surfaces of nanoporous metals and semiconductors allow one to control the wetting energies of electrolytes by electrical potentials. Thereby, it is possible to tune droplet shape and liquid spreading dynamics at surfaces, however also the imbibition into the porous surface is under external control via electrical potential-dependent curvatures of the liquid menisci within the nanopores. Moreover, the enormous Laplace pressures and fluid-solid interfacial stresses, typical of nanopore-confined liquids, induce noticeable deformations of the porous solids, and thus result in the case of electrowetting in a potential-dependent coupling of liquid capillarity with solid elasticity, i.e. electrically switchable elastocapillarity. The complex interplay of these phenomenologies (droplet shape dynamics, imbibition and deformation behaviour) have been barely explored to date. Here, it is proposed to explore experimentally the wetting dynamics of aqueous electrolytes at tailored, single-crystalline silicon surfaces traversed by a parallel array of tubular nanopores along with the intimately related elastic deformation of the solids under electrical potential control of the solid-liquid interfacial tension. Both direct and electrowetting with dielectric oxide layers at the nanopore surfaces shall be studied. The existence of precursor films, droplet spreading and imbibition dynamics as well as the deformation on the microscopic (atomic silicon lattice) and macroscopic (substrate) scale will be scrutinised by time-dependent droplet shape analysis, opto-fluidic interferometry, dilatometry and synchrotron-based in-situ x-ray diffraction under variation of the mean pore diameter and porosity of the surface. The experiments shall be analysed in close cooperation with projects in this priority program focusing on computational modelling and mesoscopic phenomenological theories for liquid spreading, imbibition and elastocapillarity at planar and porous surfaces.

The overarching objective of this project is a fundamental, predictive understanding of electrically switchable static and dynamic wetting at nanoporous surfaces.

2.3 Work programme incl. proposed research methods

In the following the work program is outlined. First we motivate the selection of monolithic nanoporous substrates and the electrolytes to be employed.

2.3.1 Selection of Nanoporous Substrates

Based on our synthesis expertise[53,54,56] nanoporous silicon shall be prepared by electrochemical etching of highly p- and n-doped and thus electrically conductive (100) silicon wafers. The resulting porous substrate have "model" pore geometries with narrow pore size distributions (10%) and tubular, non-interconnected pore shapes. This allows for a simple interpretation of the imbibition experiments and reduces the experimental challenges, since the collective movement of the menisci in the parallel array of channels, as detectable by our opto-interferometrical experiments outlined below, is representative of the movement of one meniscus in a single pore. The pore diameter is tunable by electrochemical means between 2 and 200 nm[11] and the depth of the porous layer, i.e. the membrane thickness, can be selected by appropriate etching times between 1μm and 300μm.
Moreover, the single-crystalline structure of the substrate allows one to perform detailed scattering experiments on the deformation of the atomic silicon lattice and thus on the elastic response of the solid upon traction forces induced by the infused liquid (elastocapillary effects)[8,9,69] as a function of electrowetting. Additional details regarding the nanoporous substrates are given in the description of workpackage WP-1.

2.3.2 Model electrolytes

We will use aqueous electrolytes such as KCl/water and KI/water solutions. In the kinetic experiments the salt concentration should be systematically varied (0.1 - 2 Molar) in order to study its impact on the electrowetting dynamics. Preliminary electrowetting experiments, see Fig. 1, have been performed with 2 Molar aqueous KCl solutions.
There is substantial literature data with regard to this "simple" electrolytes in planar geometries. Most theoretical consideration of electrowetting refer to these "model" electrolytes, which allows for a quantitative comparison of our experiments with literature data but also with simulation studies on electrowetting performed in other projects of the SPP. At an advanced stage of the project also the study of room-temperature ionic liquids is anticipated. The larger electrochemical window before electrolysis makes them particularly interesting for direct electrowetting experiments.

2.3.3 Work packages (WPs)

WP-1.1: Preparation of Tailored Nanoporous Substrates Electrochemical synthesis of the following nanoporous silicon substrates and selected chemical pore-surface grafting:

- free-standing membranes with diameters up to 3 cm and selected thicknesses in a range between 10 to 300 μm (adjustable by the etching time)[54]
- selected mean pore diameters of 5, 8, 10, 15 and 20 nm.
- porosities ranging from 40% to 65%
- for selected samples and EWOD experiments a dielectric oxidic pore wall will be achieved by chemical treatment (H_2O_2 solutions). The resulting hydrophilic nanopores will be silanized in

order to achieve an initial hydrophobic Cassie-Baxter state. The corresponding expertise has been established in previous projects on nanoporous silicon and silica.[59]

The necessary electrochemistry environment and porous silicon etching cells are available in the Huber group. The substrates shapes can be adapted for the specific electrowetting experiments by a Laser cutter available at TUHH.

WP-1.2: Characterisation of Tailored nanoporous solids A careful characterisation of the nanoporous substrates, in particular with regard to the specific surface area, the specific nanochannel density at the surface (porosity), the mean pore diameter is of utmost importance for the interpretation of the experiments with phenomenological models available in the literature, but also for the interaction with the modelling groups of the SPP 2171. This will be performed by the following experimental methods:

- Volumetric nitrogen adsorption at 77 K allows one to determine the porosity, pore surface area and pore size distributions.
- Scanning electron microscopy and transmission electron microscopy will performed in order to validate the sample quality.
- Atomic force microscopy will be employed to characterise the mesoscopic surface roughness of the nanoporous silicon substrates.
- Given the infrared transparency of silicon, infrared spectroscopy allows one to probe the quality of the surface-grafting, in particular the silanization of the pore-surface grafted samples[70]

WP-2: Droplet Shape and Charge Kinetics Analysis under Electrical Potential Control The static and dynamic wetting properties under electrical potential control will be performed while systematically varying the mean channel diameter, the porosity and the pore-surface grafting. The following experiments will be performed on the non-porous and porous substrates:

- **Determination of electrochemical windows**, i.e. absence of electrolysis for the model electrolytes shall be explored by cyclic voltammetry measurements for the electrolytes employed. This allows one to limit the range of applied electrical potential in the wetting regime to the purely capacitive regime, where the electrical double layer forms at the solid-liquid interface. Moreover, the potential of zero-charge shall be determined by this method, i.e. the voltage where the pore walls are completely uncharged and thus the minimal change in wetting angle is expected.[12]
- On the fully liquid saturated samples **potential-step coulometry** will be performed,[12] i.e. after applying fixed electrical potentials the current relaxation and thus the self-diffusion dynamics and formation of the electrical double layers is monitored as a function of time. This allows one to determine the surface-specific charge capacitance and to explore the limits of ion transport kinetics determining also the electro-switching kinetics both at the planar silicon substrates and in pore space.[12] These data sets will be provided to the groups performing simulation studies (Harting, Holm) in order to calibrate their models, see also individual collaborations with the SPP 2171. Moreover, it allows one to determine appropriate time-constants for possible alternating current (AC) electrowetting experiments at an advanced stage of this project.
- **Time-dependent optical analysis of the droplet shape** after depositing electrolyte droplets on the substrates for a range of electrical potentials in the available electrochemical window, in particular determination of the contact angle $\Theta(t)$, the droplet height $h(t)$ and the droplet radius $R(t)$ for the Cassie-Baxter state, the transition to the Wenzel state and the reverse

transition to the Cassie-Baxter state (wetting and dewetting transition). Possible hysteresis with respect to the potentials necessary to induce the different wetting states shall be explored in detail. The experiments will be performed at room temperature under controlled humidity conditions in the Droplet Shape Analyze DA100 available at TUHH. It is equipped with a camera recording system with a temporal resolution of 600 pictures/s.

WP-3: Imbibition Dynamics Analysis under Electrical Potential Control Extensive parameter scanning of nanopore imbibition dynamics by systematic variation of the electrowetting parameters explored in WP-1 and the variation of the pore geometry by in-situ opto-interferometric experiments.[66,67] In particular, the high spatial and temporal resolution of the interferometric experiments (in the μs and sub–μm regime), see Fig. 4 will be employed to study the initial imbibition regimes and thus the possible spreading of precursor films (before the main menisci). To this end effective medium theory has to be applied in order to achieve a full understanding of the reflected light intensities with respect to different liquid filling states (pure meniscus movement or meniscus movement $+$ precursor film spreading).[66,67]
Also, the terminal imbibition dynamics before complete filling of the membranes will be studied in detail for selected samples. For an advancement of an unbroadened imbibition front a sharp kink in the filling dynamics is expected.[59,63] By contrast, imbibition front broadening, which can result from the pore size distribution will result in a continuous approach to the completely filled state, and thus gives important information on the filling mechanisms, possible precursor film spreading in pore space.[59] Specifically, deviations from the classic Lucas-Washburn $\sqrt{t}$-scaling of the invasion kinetics, of the imbibition speed v_i will be scrutinized with regard to the occurrence of precursor-film spreading, immobile boundary layers and electrokinetic effects. For calibration of the opto-fluidic experiments also imbibition with unpolar model liquids, such as linear n-alkanes will be performed.
The necessary imbibition sample cells are available at TUHH. However, the PhD student has to adapt the sample holders for the electrowetting experiments. Particular experimentally challenging will be a proper mounting of the electrodes in the small droplets on the substrate surface during the electrowetting experiment. Here, the prospective PhD student will profit from our preliminary electrowetting experiments.

WP-4: Static and Dynamic Elastocapillarity Experiments under Electric Potential Control The impact of traction forces of the advancing and receding liquids in pore space shall be explored on the microscopic (atomic) and macroscopic scale for the nanoporous, single-crystalline matrices. The expected maximal contraction or expansion strains ϵ are expected to be a few 10^{-4}.[8]

- **Macroscopic deformation:**The macroscopic deformation of the nanoporous membranes will be explored with in-situ dilatometry, see experimental geometry in Fig.1 in a commercial Netzsch dilatometer as a function of dynamic, i.e. time-dependent electrowetting conditions, specifically for the transition between the Cassie-Baxter and the Wenzel state and vice versa. Here noticeable contractions and expansions of the membrane are expected, because of the Laplace pressures at the highly curved menisci in the pore space, see Fig. 6 and our previous publication on these Laplace-pressure induced deformations in nanoporous silicon,[8,9] measured in an analogous dilatometry geometry. Note, however, that for the configurations in Fig. 1(b) and (c) the pressure in the nanopore-confined liquid are expected to increase or descrease, respectively, from p_L at the menisci linearly to the hydrostatic pressure in the bulk droplet during the filling or emptying process. This means that for a fixed electrical-potential and thus fixed menisci radii the amount of strained solid and thus the macroscopic deformation will be a function of time. Therefore, it will be particularly interesting to relate the filling kinetics of the channels with the deformation kinetics measured.

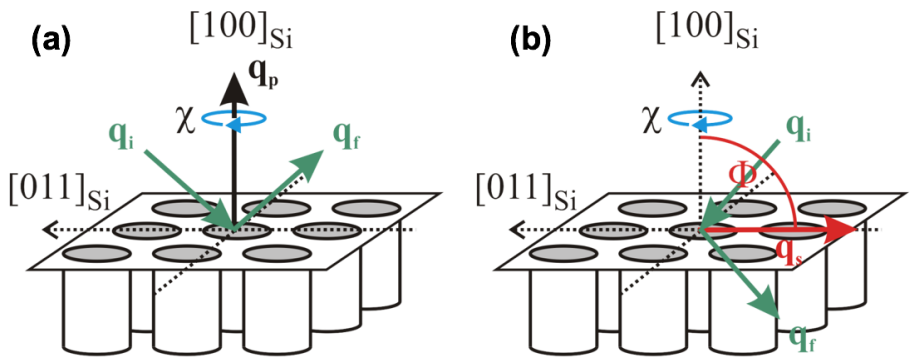

Figure 7: Kinematic scattering geometries of x-ray diffraction experiments on the microscopic deformation of a nanoporous silicon membrane. (a) Scans with scattering wave-vector transfer q_p parallel to the pore axis and thus parallel to tubular channels allow one to determine the Si-lattice strain parallel to the nanopore axis $\epsilon_{\parallel}$ (b) Wave-vector transfer q_s scans perpendicular to the pore axis allow one to determine the Si-lattice strain perpendicular to the nanopore axis $\epsilon_{\perp}$ [9,53,64]

.

- **Microscopic deformation:** For selected sample (electrical potentials, pore diameters) also synchrotron-based, high-resolution wide-angle scattering (WAXS) experiments on the atomic silicon lattice in the pore walls under in-situ electro-wetting are planned. To this end the wetting-dynamic dependent position of the (004) Bragg reflection of the crystalline silicon membrane shall be explored. As we outlined recently in a paper on elastocapillarity in tubular channels, it will be interesting to perform experiments with scattering wavevector transfer parallel to the long axis of the channels and perpendicular to the channels. This allows one to monitor anisotropic wetting strains and thus elastocapillarity effects parallel and perpendicular to the pore axis, see Fig. 7. They should significantly differ because of the anisotropic loading state of the liquid-infused nanopore arrays. These experiments will profit from a long experience in the Huber research group regarding x-ray scattering experiments on nanoporous media, in particular on nanoporous silicon.[53,57,71,72] The PhD student has to adapt available in-situ fluid diffraction cells for the in-situ electrowetting scattering experiments. Experiments at a laboratory WAXS setup, available in the Huber lab, will be performed in preparation of the synchrotron-based studies.

WP-5: Phenomenological Analysis and Comparison with Mesoscopic Models and Simulation studies, Preparation of Tutorial

- **Analysis of electrically switchable spreading and imbibition dynamics** The droplet shape and imbibition kinetics will be analysed with available phenomenological models for droplet spreading[40] and imbibition in porous media,[20,30] while considering electrically tunable surface energies. A particular emphasis will be put on possible precursor-film spreading, ahead of the main menisci in pore space and their impact on the imbibition kinetics observed in the opto-fluidic experiments and in the droplet shape evolution at the macroscopic surface. The results will be communicated to the groups performing simulation studies and mesoscopic modelling of adaptive wetting on porous surfaces (Antonyuk, Gambaryan-Roisman, Holm, Harting, Thiele), see also the planned individual collaborations in section 2.8.

- **Analysis of electrically switchable elastocapillarity** The mechanical deformation experiments will be analysed with continuum mechanics models for elastocapillarity in arrays of parallel nanochannels, recently derived in the Huber group jointly with Gennady Gor and Jörg Weißmüller.[9] The anisotropic wetting stress[9] experiments will be communicated and discussed

with SPP groups working on wetting-induced deformation of surfaces both with regard to simulation and analytical theories, see also the planned embedding of our project into the SPP 2171 in section 2.8.

- **Preparation of a tutorial on spreading, imbibition and elastocapillarity at nanoporous surfaces** A tutorial on electrically controlled wetting experiments with nanoporous media, in terms of sample preparation, experimental techniques, experimental challenges shall be written in the course of the project. The tutorial will be distributed within the SPP 2171 and shall be added as an appendix to the thesis of the PhD candidate.

2.3.4 Work package timetable

The following schedule is foreseen for the workpackages outlined above:

Months	1-6	7-12	13-18	19-24	25-30	31-36
WP-1: Synthesis and Characterization of Tailored Nanoporous Substrates	■	■	■			
WP-2: Droplet Shape and Charge Kinetics Analysis under Electrical Potential Control	■	■	■	■		
WP-3: Imbibition Dynamics Analysis under Electrical Potential Control		■	■	■	■	■
WP-4: Static and Dynamic Elastocapillarity Experiments		■	■	■	■	■
WP-5: Phenomenological analysis and comparison with mesoscopic models and simulation studies			■	■	■	■

Figure 8: Work package timetable

2.4 Data handling

Obtained data will be archived in an online repository (e.g. Dryad), to which will be referred in resulting publications. This will allow other researchers to validate or compare the data or perform further analyses.

2.5 Descriptions of proposed investigations involving experiments on humans, human materials or animals as well as dual use research of concern

Not applicable.

2.6 Other information

Not applicable.

2.7 Information on scientific and financial involvement of international cooperation partners

Not applicable.

2.8 Information on scientific cooperation within SPP 2171

Subject Matter: The subject matter of our project fits well with several goals of the SPP 2171: Our project aims at a deeper understanding of the fundamental physics behind dynamic electrowetting phenomena at electrically switchable porous substrates. In particular it will provide useful experimental data for model porous media with well-defined geometry and known fluid-solid interactions, and thus valuable data for an analysis with analytical mesoscopic hydrodynamic models as well as simulation studies. It addresses simple aqueous electrolytes and aims at the exploration of reversible, switchable liquid wetting dynamics. Given the importance of silicon as an archetypical material in micro- and nanofluidics and the increasing relevance of nanoporous solids in combination with electrolytes in a huge variety of technologies ranging from bio-sensing to energy storage and harvesting [11] our study will likely also provide important fundamental base knowledge for future technological applications of electrowetting employing nanoporous media. Moreover, the traction forces of the liquid on the solid (specifically the Laplace pressures) can induce noticeable elastic deformations of the stiff solid and allow therefore to explore the coupling of solid elasticity to liquid capillarity, another main research focus of the SPP 2171, and this in an electrical-potential controlled manner.

Organisation: We will compare our findings on electro-switchable surfaces with the results of other groups employing alternative means for switchable surface energies and alternative planar or porous wetting geometries. We also offer our substantial experimental expertise with regard to the characterisation of porous media [56] as well as extensive knowledge on, and experimental equipment for the study of, imbibition kinetics in porous media. It is planned that the prospective PhD student prepares a tutorial on electrowetting experiments with nanoporous media that shall be distributed in the SPP. Moreover, we would be happy to prepare and provide nanoporous silicon samples for other experimental groups of the SPP 2171. Based on personal knowledge of potential project leaders and an exchange of ideas before proposal submission, we are foreseeing the following individual collaborations with theoretically (T) and experimentally (E) working research groups:
(T1) Project "Mesoscopic Gradient Dynamics for the (De)Wetting Dynamics on Adaptive Substrates": We will collaborate with the **Thiele** group (Münster) with regard to the validation of mesoscopic continuum wetting models [73,74] for porous surfaces that adapt their wettability. In particular, we will provide measured static droplet shape profiles and experimental data on the droplet spreading kinetics and nanopore imbibition kinetics as a function of the porosity, of the pore-surface graftings and electrical potentials, and thus electrically tunable wetting energies (WP-5). The thin-film gradient models could also be of specific interest with regard to the study of thin liquid precursor films in the nanochannels.
(T2) Project "Dynamical Electro-Wetting Behaviour of Functionalised Charged Surfaces": We intend to collaborate with the **Holm** group (Stuttgart) with regard to the parameterisation and validation of Lattice Boltzmann Electro Kinetics (LB-EK) models with implicitly dissolved solvent and ions. [75,76] We will provide measured static droplet shape profiles and experimental data on the electrokinetics (electrical capacitance, ion sorption kinetics) (WP-2), droplet spreading kinetics (WP-3) and nanopore imbibition kinetics (WP-3) as a function of electrically tunable wetting energies, both for the non-porous and nanoporous silicon surfaces. A direct comparison of our experiments with their simulations will allow us to achieve detailed, microscopic insights in the dynamic electrowetting at our nanoporous model surfaces (WP-5). Whereas we produce integral quantities, the Holm group can provide spatially resolved ion concentrations and the electrical potential everywhere in the drop and in the confined liquid.
(T3) Project Harting: We will collaborate with the **Harting** group (FZ Juelich/Erlangen) on liquid imbibition in porous media. We will provide experimental data for coupled multiphase Lattice-Boltzmann and Nernst-Planck solver [77,78] (WP-2, WP-3, WP-5). Depending on the progress in our project, we think also about studying nanoparticle-loaded electrolytes at an advanced state of

our project. Here, we could profit from the strong expertise of this group regarding modelling of nanoparticle flow by Lattice Boltzmann techniques. The nanoparticles could be provided by the group of **Guerevich** (Bochum).
(T4) Project "Modelling of Spreading, Imbibition and Evaporation of Liquids on Deformable Porous Substrates": We agreed with the **Gambaryan-Roisman** group (Darmstadt) that we will provide data sets on our imbibition experiments regarding a model nanoporous medium with well-defined pore geometry to calibrate and validate the mesoscopic models for imbibition in porous media[22] employed in this project (WP-2, WP-3, WP-5). The consideration of disjoining pressures and possible transport contributions of fluid via the vapour phase (evaporation) in the models used in this group will be of high relevance for our dynamic electrowetting experiments on nanoscale pore structures.
(E1) Project "Photo-Switchable Surfaces to Manipulate Adsorbed Liquid Droplets": We intend to cooperate with the **Santer** group (Potsdam). Ms. Santer is an expert in photo-switchable polymer graftings, specifically also of silicon surface-graftings.[79] With her expertise we will try to introduce photo-switchable wetting energies into our silicon nanochannels at an advanced state of the project (WP-1).
(E2) Project "Dynamics of the coupled interaction of the three-phase contact line with electrokinetic and electrochemical processes on switchable surfaces": We intend to cooperate with the **Schönecker** group (Kaiserslautern) with regard to their electrowetting experiments. We will provide nanoporous silicon membranes as electrode materials for their H_2-induced droplet movement experiments (WP-1). Vice versa, we are going to study the imbibition dynamics and electrochemical characteristics of nanoporous gold employed as electrodes in their electrowetting experiments, based on our expertise with nanoporous metallic systems, specifically cyclic voltammetry on these materials[12] (WP-2, WP-3, WP-5).
Finally, we will actively participate in the planned SPP events (workshops and Advanced Schools) both on Principal Investigator and PhD student level and applied for the corresponding financial support (see requested funding).

3 Bibliography

[1] Quilliet, C.; Berge, B. *Current Opinion In Colloid & Interface Science* **2001**, *6*, 34–39.
[2] Mugele, F.; Baret, J. C. *J. Phys.: Condens. Matter* **2005**, *17*, R705–R774.
[3] Bonn, D.; Eggers, J.; Indekeu, J.; Meunier, J.; Rolley, E. *Reviews of Modern Physics* **2009**, *81*, 739–805.
[4] Chen, C.; Lu, K. J.; Li, X. F.; Dong, J. F.; Lu, J. T.; Zhuang, L. *RSC Adv.* **2014**, *4*, 6545–6555.
[5] Monroe, C. W.; Daikhin, L. I.; Urbakh, M.; Kornyshev, A. A. *Physical Review Letters* **2006**, *97*, 136102.
[6] Darhuber, A. A.; Troian, S. M. *Annual Review of Fluid Mechanics* **2005**, *37*, 425–455.
[7] Lippmann, G. *Ann. Chim. Phys* **1875**, *5*, 494.
[8] Gor, G. Y.; Bertinetti, L.; Bernstein, N.; Hofmann, T.; Fratzl, P.; Huber, P. *Applied Physics Letters* **2015**, *106*, 261901.
[9] Gor, G. Y.; Huber, P.; Weissmuller, J. *Physical Review Materials* **2018**, *2*, 086002.
[10] Nowak, J. Electrowetting on Nanoporous Silicon. M.Sc. thesis, Hamburg University of Technology, 2018.
[11] Canham, L., Ed. *Handbook of Porous Silicon*; Springer, 2015.
[12] Xue, Y.; Markmann, J.; Duan, H. L.; Weissmueller, J.; Huber, P. *Nat. Commun.* **2014**, *5*, 4237.
[13] Chen, X. D.; Hirtz, M.; Fuchs, H.; Chi, L. F. *Advanced Materials* **2005**, *17*, 2881–+.
[14] Chibbaro, S. *Eur. Phys. J. E* **2008**, *27*, 99.
[15] Engel, M.; Stühn, B. *J. Chem. Phys.* **2010**, *132*, 224502.
[16] Stone, H. A.; Stroock, A. D.; Ajdari, A. *Annu. Rev. Fluid Mech.* **2004**, *36*, 381.

[17] Karniadakis, G.; Beskok, A.; Aluru, N. *Microflows and Nanoflows: Fundamentals and Simulation*; Springer: New York, 2005.
[18] Schoch, R. B.; Han, J.; Renaud, P. *Rev. Mod. Phys.* **2008**, *80*, 839.
[19] Persson, F.; Thamdrup, L. H.; Mikkelsen, M. B. L.; Jaarlgard, S. E.; Skafte-Pedersen, P.; Bruus, H.; Kristensen, A. *Nanotechnology* **2007**, *18*, 245301.
[20] Seveno, D.; Ledauphin, V.; Martic, G.; Voue, M.; De Coninck, J. *Langmuir* **2002**, *18*, 7496–7502.
[21] Frank, X.; Perre, P. *Physics of Fluids* **2012**, *24*, 042101.
[22] Gambaryan-Roisman, T. *Current Opinion In Colloid & Interface Science* **2014**, *19*, 320–335.
[23] de Gennes, P. G.; Brochard-Wyart, F.; Quere, D. *Capillarity and Wetting Phenomena: Drops, Bubbles, Pearls, Waves*; Springer: New York, 2004.
[24] Kriel, F. H.; Sedev, R.; Priest, C. *Isr. J. Chem.* **2014**, *54*, 1519–1532.
[25] Lucas, R. *Kolloid Zeitschrift* **1918**, *23*, 15.
[26] Washburn, E. W. *Phys. Rev.* **1921**, *17*, 273.
[27] Gruener, S.; Hofmann, T.; Wallacher, D.; Kityk, A. V.; Huber, P. *Phys. Rev. E* **2009**, *79*, 067301.
[28] van Delft, K. M.; Eijkel, J. C. T.; Mijatovic, D.; Druzhinina, T. S.; Rathgen, H.; Tas, N. R.; van den Berg, A.; Mugele, F. *Nano Lett.* **2007**, *7*, 345.
[29] Vincent, O.; Szenicer, A.; Stroock, A. D. *Soft Matter* **2016**, *12*, 6656–6661.
[30] Gruener, S.; Huber, P. *Transport in Porous Media* **2018**, *(in press)*.
[31] Dimitrov, D. I.; Milchev, A.; Binder, K. *Phys. Rev. Lett.* **2007**, *99*, 054501.
[32] Gelb, L. D.; Hopkins, A. C. *Nano Lett.* **2002**, *2*, 1281.
[33] Ahadian, S.; Kawazoe, Y. *Colloid Polym. Sci.* **2009**, *287*, 961.
[34] Stukan, M. R.; Ligneul, P.; Crawshaw, J. P.; Boek, E. S. *Langmuir* **2010**, *26*, 13342–13352.
[35] Bakli, C.; Chakraborty, S. *Appl. Phys. Lett.* **2012**, *101*, 153112.
[36] Rauscher, M.; Dietrich, S. *Annu. Rev. Mater. Res.* **2008**, *38*, 143–172.
[37] Bocquet, L.; Tabeling, P. *Lab Chip* **2014**, *14*, 3143–58.
[38] Vo, T. Q.; Kim, B. *Scientific Reports* **2016**, *6*, 33881 EP –.
[39] de Gennes, P. G. *Rev. Mod. Phys.* **1985**, *57*, 827.
[40] Thiele, U. *Colloids and Surfaces A-physicochemical and Engineering Aspects* **2018**, *553*, 487–495.
[41] Lu, G.; Wang, X.-D.; Duan, Y.-Y. *Coll. Surf. A - Physicochem. Eng. Aspects* **2013**, *433*, 95–103.
[42] Quéré, D. *Europhys. Lett.* **1997**, *39*, 533–538.
[43] Zhu, L. B.; Xu, J. W.; Xiu, Y. H.; Sun, Y. Y.; Hess, D. W.; Wong, C. P. *Journal of Physical Chemistry B* **2006**, *110*, 15945–15950.
[44] Han, Z. J.; Tay, B.; Tan, C. M.; Shakerzadeh, M.; Ostrikov, K. *Acs Nano* **2009**, *3*, 3031–3036.
[45] Gor, G. Y.; Huber, P.; Bernstein, N. *Applied Physics Reviews* **2017**, *4*, UNSP 011303.
[46] Andreotti, B.; Baumchen, O.; Boulogne, F.; Daniels, K. E.; Dufresne, E. R.; Perrin, H.; Salez, T.; Snoeijer, J. H.; Style, R. W. *Soft Matter* **2016**, *12*, 2993–2996.
[47] Duprat, C.; Aristoff, J. M.; Stone, H. A. *Journal of Fluid Mechanics* **2011**, *679*, 641–654.
[48] Karpitschka, S.; Das, S.; van Gorcum, M.; Perrin, H.; Andreotti, B.; Snoeijer, J. H. *Nature Communications* **2015**, *6*, 7891.
[49] Zhao, M. H.; Lequeux, F.; Narita, T.; Roche, M.; Limat, L.; Dervaux, J. *Soft Matter* **2018**, *14*, 61–72.
[50] Guenther, G.; Prass, J.; Paris, O.; Schoen, M. *Phys. Rev. Lett.* **2008**, *101*, 086104.
[51] Grosman, A.; Puibasset, J.; Rolley, E. *Epl* **2015**, *109*, 56002.
[52] Kvick, M.; Martinez, D. M.; Hewitt, D. R.; Balmforth, N. J. *Physical Review Fluids* **2017**, *2*, 074001.
[53] Henschel, A.; Hofmann, T.; Huber, P.; Knorr, K. *Phys. Rev. E* **2007**, *75*, 021607.
[54] Gruener, S.; Huber, P. *Phys. Rev. Lett.* **2008**, *100*, 064502.

[55] Kumar, P.; Hofmann, T.; Knorr, K.; Huber, P.; Schreib, P.; Lemmens, P. *J. Appl. Phys.* **2008**, *103*, 024303.
[56] Huber, P. *J. Phys.: Cond. Matt.* **2015**, *27*, 103102.
[57] Sentker, K.; Zantop, A. W.; Lippmann, M.; Hofmann, T.; Seeck, O. H.; Kityk, A. V.; Yildirim, A.; Schonhals, A.; Mazza, M. G.; Huber, P. *Physical Review Letters* **2018**, *120*, 067801.
[58] Kumar, P.; Franzese, G.; Stanley, H. E. *Phys. Rev. Lett.* **2008**, *100*, 105701.
[59] Gruener, S.; Hermes, H. E.; Schillinger, B.; Egelhaaf, S. U.; Huber, P. *Colloids and Surfaces A-physicochemical and Engineering Aspects* **2016**, *496*, 13–27.
[60] Huber, P.; Gruener, S.; Schaefer, C.; Knorr, K.; Kityk, A. V. *Eur. Phys. J. Special Topics* **2007**, *141*, 101–105.
[61] Gruener, S.; Huber, P. *Phys. Rev. Lett.* **2009**, *103*, 174501.
[62] Gruener, S.; Huber, P. *J. Phys. Cond. Matter* **2011**, *23*, 184109.
[63] Gruener, S.; Sadjadi, Z.; Hermes, H. E.; Kityk, A. V.; Knorr, K.; Egelhaaf, S. U.; Rieger, H.; Huber, P. *Proceedings of the National Academy of Sciences of the United States of America* **2012**, *109*, 10245–10250.
[64] Kusmin, A.; Gruener, S.; Henschel, A.; Holderer, O.; Allgaier, J.; Richter, D.; Huber, P. *Journal of Physical Chemistry Letters* **2010**, *1*, 3116–3121.
[65] Kusmin, A.; Gruener, S.; Henschel, A.; de Souza, N.; Allgaier, J.; Richter, D.; Huber, P. *Macromolecules* **2010**, *43*, 8162–8169.
[66] Busch, M. Optische Untersuchungen zum Kapillarsteigen in mesoporoesen Festkoerpern. M.Sc. thesis, Saarland University, 2012.
[67] Urteaga, R.; Acquaroli, L. N.; Koropecki, R. R.; Santos, A.; Alba, M.; Pallares, J.; Marsal, L. F.; Berli, C. L. A. *Langmuir* **2013**, *29*, 2784–2789.
[68] Bangham, D.; Fakhoury, N. *Nature* **1928**, *122*, 681–682.
[69] Dolino, G.; Bellet, D.; Faivre, C. *Phys. Rev. B* **1996**, *54*, 17919–17929.
[70] Wallacher, D.; Huber, P.; Knorr, K. *J. Low Temp. Phys.* **1998**, *113*, 19.
[71] Henschel, A.; Huber, P.; Knorr, K. *Phys. Rev. E* **2008**, *77*, 042602.
[72] Kusmin, A.; Gruener, S.; Henschel, A.; Holderer, O.; Allgaier, J.; Richter, D.; Huber, P. *Journal of Physical Chemistry Letters* **2010**, *1*, 3116–3121.
[73] Thiele, U.; Snoeijer, J.; Trinschek, S.; John, K. *Langmuir* **2018**, *35*, 7210–7221.
[74] Thiele, U. *Colloids Surf. A* **2018**, *553*, 487–495.
[75] Rempfer, G.; Davies, G. B.; Holm, C.; de Graaf, J. *Journal of Chemical Physics* **2016**, *145*, 044901.
[76] Kuron, M.; Rempfer, G.; Schornbaum, F.; Bauer, M.; Godenschwager, C.; Holm, C.; de Graaf, J. *Journal of Chemical Physics* **2016**, *145*, 214102.
[77] Rivas, N.; Harting, J. *Submitted for publication*.
[78] Rivas, N.; Harting, J. *arXiv:1805.01351, submitted for publication*.
[79] Malyar, I. V.; Titov, E.; Lomadze, N.; Saalfrank, P.; Santer, S. *Journal of Chemical Physics* **2017**, *146*, 104703.

4 Requested modules/funds

4.1 Basic Module

4.1.1 Funding for staff

We apply for a funding of a PhD student position (TV-L 13, 75%) for 36 months. She or he should perform the work packages WP-1 to WP-5.

4.1.2 Equipment up to €10,000, Software and Consumables

Chemicals for the electrochemical nanoporous silicon preparation:	3000 €
Nitrogen (for sorption isotherm measurements), solvents, glassware:	2000 €
Highly *p*- and *n*-doped silicon wafers for the electrochemical preparation of porous silicon substrates:	6000 €
Parts for the electrowetting sample holders for the opto-fluidic studies:	3000 €
Expenses for the usage of the electron microscopes (SEM and TEM) of the Gerätezentrum "Elektronenmikroskopie" at TUHH:	5000 €
Subtotal:	**19000** €

4.1.3 Travel Expenses

1st and 2nd year, SPP workshop (4 days), PI & PhD student present	1040 €
1st year Advanced school, PhD student present	600 €
2nd year PhD candidate workshop	520 €
3rd year international conference - everyone should be present (5 days)	1200 €
1 international scientific conference (abroad)/year - 3x1500€	4500 €
Subtotal:	**7860** €

4.1.4 Project-related publication expenses

1800 € for open access publications.

5 Project requirements

5.1 Employment status information

Patrick Huber: tenured Professor (W2) at Hamburg University of Technology

5.2 Composition of the project group

1) Kathrin Sentker (physicist, PhD student, full time, funded by TUHH): support in nanoporous silicon preparation, opto-interferometrical experiments
2) Rainer Behn (engineer, full time, funded by TUHH): maintenance of opto-interferometrical and x-ray diffraction setups

5.3 Researchers with whom you have collaborated scientifically within the past three years

M. Deutsch, Bar-Ilan University (Israel); P. Fratzl, Potsdam; O. Gang, Columbia University;T. Hofmann, Berlin; D. Morineau, Rennes (France); B. Ocko, Brookhaven National Lab (USA); A. Schönhals, Berlin; M. Steinhart, Osnabrück; U. Volkmann, Santiago de Chile; R. Wehrspohn, Halle; J. Weissmueller, Hamburg

5.4 Scientific equipment

- Volumetric gas adsorption isotherm setup (Quantachrome autosorb iQ)
- Droplet shape analyzer (Krüss DSA100)
- X-ray diffraction (Bruker D8 Advance (WAXS) and Bruker Nanostar (SAXS))
- Setup for interferometric, time-dependent imbibition experiments, self-built
- Dilatometer with horizontal sample geometry for electrowetting (Netzsch DIL 402C)
- Potentiostat for electrokinetic measurements (Autolab Potentio-/Galvanostat)
- Atomic Force Microscope (JPK-Bruker Nanowizard)